Investigation of the influence of Ni and Cu additions on the wear behaviour of spray formed Al-15Si alloy at elevated temperatures

Mehabubsubahani R. Alavandi[1], Julfikar Haider[2] and Dayanand M. Goudar[1,*]

[1]Department of Mechanical Engineering, Tontadarya College of Engineering, GADAG, India, 582101

[2]Department of Engineering, Manchester Metropolitan University, Chester Street, Manchester, M1 5GD, UK

***Corresponding Author:**

Professor Dayanand M. Goudar

Email: dmgoudartce@gmail.com

Abstract

The aim of this study is to develop a novel class of alloy material using spray forming process, which is a rapid solidification process that produces refined, equiaxed microstructures with low segregation. In the present study, the effects of adding Ni and Cu on the dry sliding wear behavior of the spray formed Al-15Si alloy at different elevated temperatures were investigated and compared with the cast Al-15Si alloy. Al-15Si and Al-15Si-4Ni-2Cu alloys were prepared by spray forming and conventional casting methods. The microstructure of the alloys was examined using optical and scanning electron microscopy (SEM) and energy dispersive X-rays. The hardness was measured using a Vickers hardness tester. Dry sliding wear tests at room temperature, 25°C, 100°C, 200°C, and 300°C were performed on a pin-on-disc tribometer at different loads (10, 20, 30, 40, 50 N) and a sliding velocity of 1.0 m/s. The microstructure of the spray-formed Al-15Si-4Ni-2Cu alloy show fine, spherical form of primary Si, eutectic Si phases and fine dispersion of intermetallic particles. The spray-formed alloys display higher hardness values compared to the cast alloys and the spray formed Al-15Si-4Ni-2Cu alloy show a hardness almost 24% higher than the spray formed binary alloy. Lower wear rate and coefficient of friction were obtained in the Al-15Si-4Ni-2Cu alloy at all the normal loads and elevated temperatures. The spray formed alloys emerge as a better wear resistant material than the cast alloys at elevated temperatures. Although oxidative, abrasive and delamination wear mechanisms were found in the alloys manufactured by both the technique but severe plastic deformation was observed only in the cast alloys.

Keywords

Al-Si-Ni-Cu alloy, Spray-forming, Microstructure, Intermetallic, Sliding wear, Coefficient of friction.

1. Introduction

Hypereutectic Al-Si alloy is one of the most commonly used materials in automotive and aerospace applications. Due to its outstanding properties such as low weight, oxidation and corrosion resistance, machinability as well as high damping capacity. Properties of the Si enhanced Al-Si alloy include low coefficient of thermal expansion, low density, high rigidity, hot tear strength and improved mold feeding properties. Increased Si in the Al-Si alloy results in improved castability, and melt flow ability [1]. The size, shape and distribution of hard Si particles have a significant impact on the wear behavior of hypereutectic Al-Si alloys [2]. Most hypoeutectic and eutectic Al-Si cast alloys are designed for optimal performance at temperatures below 250°C and are rarely used in practice (above 250°C) [3]. Poor mechanical and wear properties are driven by coarse Si phases at high temperatures, unstable strengthening mechanisms, incompatible lattices in the Al solid solution, and a large mismatch in lattice coherence [4]. Superior materials will play an increasingly important role in the development of advanced engineering techniques.

Multicomponent Al-Si alloys are widely used as piston materials, and demands for high performance of these alloys have increased. Improving the properties of Al-Si alloys, particularly at high temperatures, has drawn much attention to the addition of transition metals to improve the properties of the Al-Si alloy. Iron, manganese, nickel, copper and magnesium can be beneficial in improving the thermal stability of the Al-Si alloy. However, most of the alloying elements have low solid solubility in Al except Mg and Cu. During casting of an aluminum alloy, equilibrium and non-equilibrium processes lead to the formation of a variety of intermetallic phases with intricate morphologies. These intermetallic compounds have the chemical formulae Mg_2Si, Al_2Cu, Al_3Ni, Al_3CuNi, and Al_7Cu_4Ni, Al_2CuMg [5]. In recent years, numerous investigations have been carried out to investigate the influence of different alloying elements on the hardness and wear resistance of Al alloys [6]. According to previous studies [7-8], nickel is the most effective component for improving the elevated temperature properties of the Al-Si alloys. Yamanoglu et al. [8] studied the microstructure and the wear behavior of pure Al alloy with the addition of Ni. It was observed that wear resistance increased with increasing Ni content of up to 3.0 wt. % and inclined to decrease at 4 wt.% Ni. Das et al. [9] reported that the addition of 1.0 wt.% Cu to an Al-Si alloy increased wear resistance through protective surface layer strength and stability, which in turn increases the transition load from light wear to heavy wear by 3 to 4 times. However, the addition of more than 2 wt.% Cu did not affect the transient load and wear resistance of the hypereutectic Al-Si alloys [10]. According to Li et al. [11] the presence of Al_3Ni, Al_3CuNi and Al_7Cu_4Ni phases has a much higher contribution to the

properties of the Al-Si-Cu-Ni alloy at elevated temperatures due to their better thermal stability. Dwivedi [12] reported that the addition of Cu, Ni and Mg elements increases the hardness and the adhesive wear resistance of the cast Al-Si alloy. According to Jeong et al. [13], the eutectic A-Si alloy showed finer microstructure and more uniform precipitation with increasing Cu and Ni concentrations.

Funda et al. [14] studied wear behavior of Al-Ni alloys and found that increasing the Ni content up to 3.0 wt. % reduces the wear rate of the alloy. However, further increasing the Ni content increases the wear rate. Farag et al. [15] studied the mechanical and tribological properties of Al-Si-Ni alloys. It was concluded that the improvement in hardness and wear resistance is attributed to the presence of the hard primary Si phase, eutectic phase and the Al_3Ni intermetallic phase in the Al-Si-Ni alloy. The hard Al_3Ni intermetallic phase modifies the microstructure and reduces the spacing between flakes in Si and is believed to improve the wear resistance of Al-Si-Ni alloys. According to Yang et al. [16], increasing the Cu content in the Al-Si-Cu-Ni alloy leads to a change in the morphologies of Ni-rich intermetallic compounds from short strip-like to net-like and then to an annular or semi-annular shape, which has a significant impact on the mechanical properties of the alloy. Kaya et al. [17] reported that the addition of 2 wt. % Ni to the Al-12.6Si alloy results in a finer Si phase with reduced spacing between the lamellae and modified microstructure properties, resulting in an improvement in hardness. Badr et al. [18] investigated microstructure and tribological properties of Al0.1Mg-0.35Ni based alloys. It was observed that the alloy's wear resistance increases with an increase in Si content and the presence of Al_3Ni phase. Samuel et al. [19] studied the microstructures and mechanical properties of Al-Cu-Si (-Ni) alloys with conventional A319 alloy. It has been observed that the refined microstructure with dispersed Ni intermetallic particles formed in the cast Al-Cu-Si-Ni alloys provides improved elevated temperature properties. During conventional solidification processing routes, the addition of transition elements leads to the formation of coarse intermetallic phases. To improve mechanical and wear properties, the rapid solidification process is used to produce higher alloyed compositions. The finer dispersion of intermetallic Ni particles would be required to achieve the efficient strengthening of the Al-Si alloys [20].

Al-Si alloys alloyed with transition elements are produced using a rapid solidification processing route that retains more solute elements in the solid solution, and the resulting supersaturated solid solutions exhibit high thermal stability. Spray-forming is a process for producing rapidly solidified alloys and composites directly from molten metal. In this process, micro-size droplets are generated from a stream of molten metal atomization using an inert gas, and the droplets are deposited onto a substrate. The rapid solidification effects in the spray deposition process due to

the high heat exchange rate at the droplet-gas interface and also at the deposition surface ensure significant chemical and microstructural homogeneity of the pre-form [21]. The sprayed materials have fine, uniform and equiaxed microstructures; low micro segregation; high solubility; and excellent workability. During the rapid solidification process, Al alloys containing transition metals are expected to precipitate fine intermetallic compounds, resulting in high strength and increased wear resistance at room and elevated temperatures. Upadhyaya et al. [22] concluded that the superior wear properties of the spray-formed alloy are due to the reduced spacing between the particles of the intermetallic phases and changes in the microstructure of the eutectic phases.

Numerous research publications show that the addition of alloying elements Cu, Mg, Fe, etc. affects the wear resistance of Al-Si cast alloys both at room temperature and at elevated temperatures. Most of the previous studies on Ni-added Al alloys focused on the evaluation of microstructure and mechanical properties. Limited information is available in the open literature about the effect of the Ni content on the wear behavior of the hypereutectic Al-Si alloy with Cu alloy addition. In order to reduce weight and increase efficiency in the automotive and aerospace industries, rapid solidification in combination with the addition of alloying elements may produce refined structural characteristics and outstanding wear qualities at high temperatures. In this work, both Al-5Si and Al-15Si-4Ni-2Cu alloys were fabricated by a novel spray forming methods to achieve a unique microstructure leading to significantly improved elevated-temperature wear characteristics. The microstructure and wear behavior of spray formed alloys were studied at room and elevated temperatures and compared to conventionally cast alloys.

2. Experimental procedures

2.1. Materials and casting procedure

As received (Fenfee Metallurgical**,** Bangalore) ingots of cast hypereutectic A-15 Si (AC1) and Al-15Si-4Ni-2Cu (AC2) alloys were remelted in an electric furnace (Make: SILICARB Recrystallized (P) Ltd. Bangalore, India) and the super-heated molten metal poured into a preheated steel die to produce cylindrical bars (Figure 1). The composition of the experimental alloys was analyzed using an optical emission spectrometer and given in Table 1.

Figure 1. Die cast Al-15Si-4Ni-2Cu alloy

Table 1. Chemical compositions of Al-15Si and Al-15Si-4Ni-2Cu alloys (wt.%)

Alloy (alloy name)	Si	Ni	Cu	Fe	Mg	Mn	Al
Al-15Si (AC1)	15.02	---	0.02	0. 05	0.001	0.001	Bal.
Al-15Si-4Ni-2Cu (AC2)	15.00	4.01	2.10	0.007	0.0011	-	Bal.

The experimental set-up employed for the spray atomization and deposition process was used in the present investigation is shown in Figure 2(a). Figure 2(b) shows the convergent-type free-fall nozzle used in the present study. The atomization assembly consisted of a free-fall nozzle; a melt feed tube and a nozzle heater. A melt delivery made up of a ceramic tube having a inner diameter of 4 mm was inserted into the steel tube. The free-fall atomizer (nozzle) was attached to the other end of the delivery pipe in such a way that the axis of the metal delivery pipe runs through the geometric point of the atomizer. The concentric gas jets interacting with the liquid flow create instability due to the shearing action of the gas flow and its relative velocity, which leads to the disintegration of the liquid. The atomized fine droplets were deposited on a substrate held at a predetermined distance from the nozzle. The droplet spray is deposited layer by layer on the copper substrate and eventually builds up into a bell-shaped preform. The experimental set-up consists of a melting unit, an atomization assembly, a gas supply assembly and a deposition substrate. The melting unit consists of a melting furnace of 5 kg capacity and a maximum temperature of 1250ºC. The details of the spray-forming process parameters used in the present study are listed in Table 2.

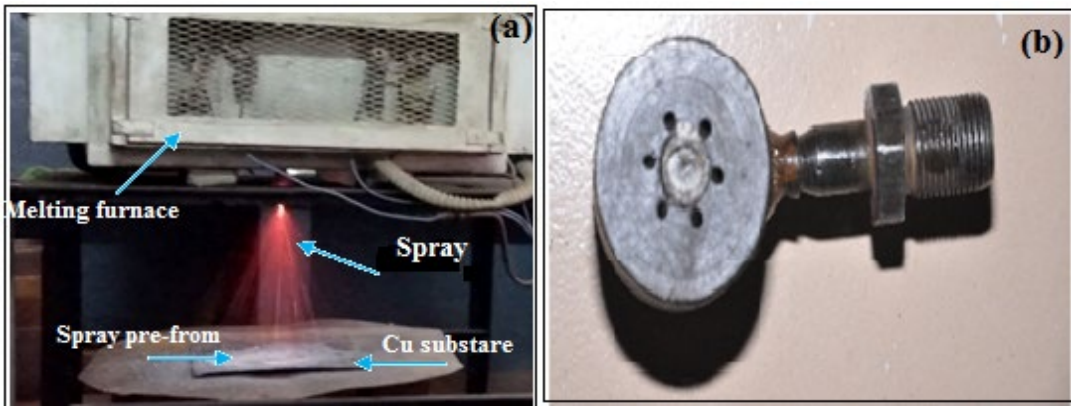

Figure 2 (a). Experimental set-up of spray deposition process and (b) Convergent type free fall nozzle [23].

Figures 3 shows the top view of the entire deposit as well as cross-sectional views after cutting the deposit into two halves. It is observed that the centre of the deposit has the greatest thickness and it decreases away from the centre.

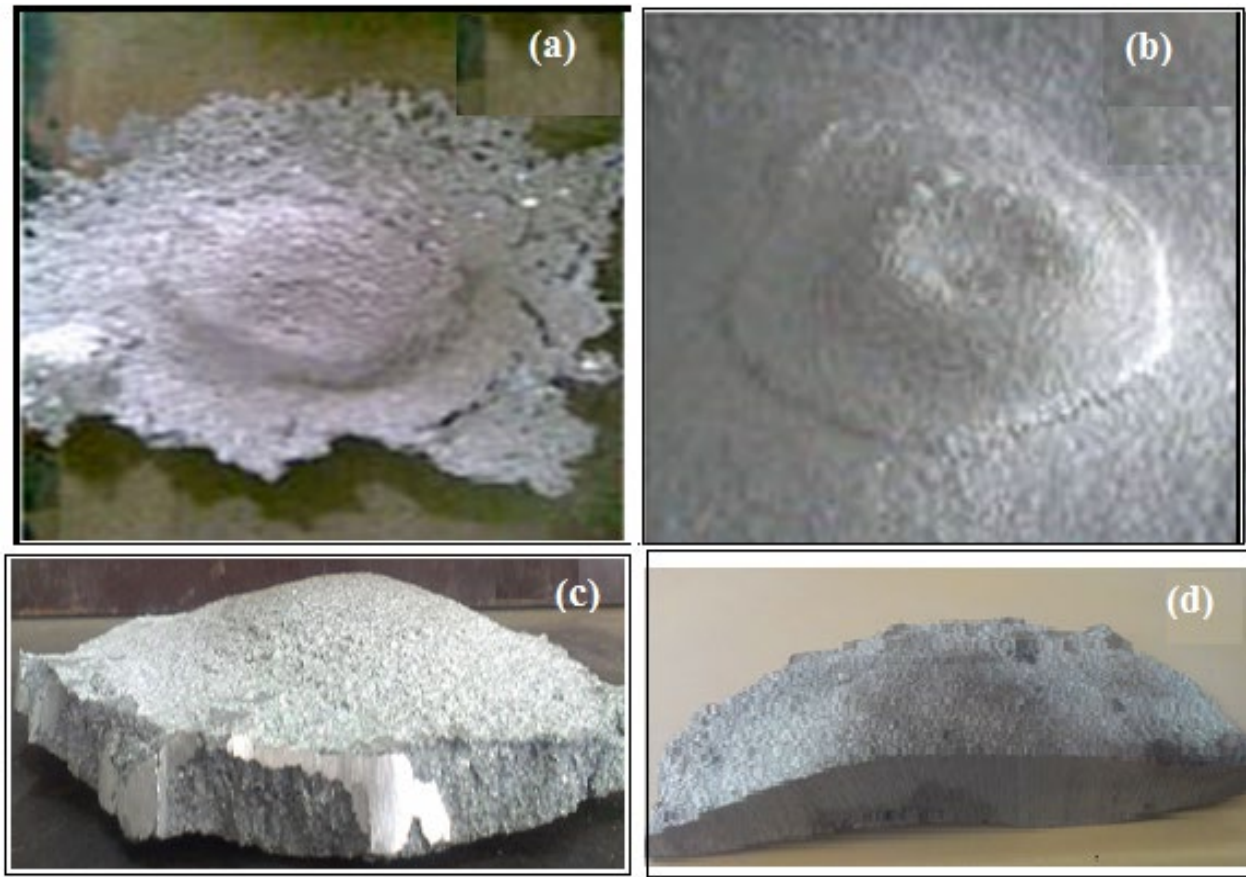

Figure 3. Pre-form images of spray- formed alloys including top views of (a) of Al-15Si (b) Al-15Si-4Ni-2Cu alloy and sectional views of (c) Al-15Si and (d) Al-15Si-4Ni-2Cu alloys

Table 2. Details of spray forming process parameters used in preparing alloy samples.

Process parameters	Al-15Si Alloy	Al-15Si-4Ni-2Cu alloy
Melting superheat temperature	825°C	950°C

Atomizing gas	Nitrogen	Nitrogen
Gas pressure (Kg/cm^2)	4.0	4.0
Atomizer-substrate distance (mm)	390	400
Melt flow rate (Kg/min)	2.45	2.5

2.2. Microstructural and hardness characterisation

Standard metallographic techniques were used to prepare samples for microstructural analyses. The samples were sectioned to a convenient size and is mounted in a homogeneous liquid mixture of resin and catalyst by the cold mounting method (Figure 4) to facilitate handling, grinding, and polishing steps. The samples were polished on emery papers with 1/0, 2/0, 3/0 and 4/0 specifications. The micro polishing was carried out on a double-disc grinding and polishing machine (Metatech DM-2T). Mirror polishing was carried out using Levi-Gated liquid alumina on a velvet cloth, and diamond paste (0.5-2µm) on a PSA-coated velvet cloth with Aero-spray. The methanol washed polished samples were etched with Keller's reagent (1% vol. hydrofluoric acid, 15% vol. hydrochloric acid, 2.5%vol. nitric acid and water). Metallographic observations were performed using an optical light microscope (ZYNAX and Clemex image analysis system) and a field emission scanning electron microscope (SEM/EDS) (JEOL JSM-6480LV). The chemical compositions of the constituent phases are examined using an energy dispersive X-ray (EDX) and SEM was operated at an acceleration voltage of 10-30 kV. The Vickers hardness test was carried out according to ASTM E384 standard. Digital Micro Vickers Hardness Tester (Future Tech Japan: FM-310) was employed to evaluate the micro-hardness of the cast and spray-formed alloys, where the experiments were conducted at an indentation load of 200g for a dwell time of 15s. An indentation depth in each measured specimen was quantified using a microscope. An average of six measurements taken from different locations on each specimen, and the average value along with the standard deviation are reported as the ultimate hardness value of the alloys.

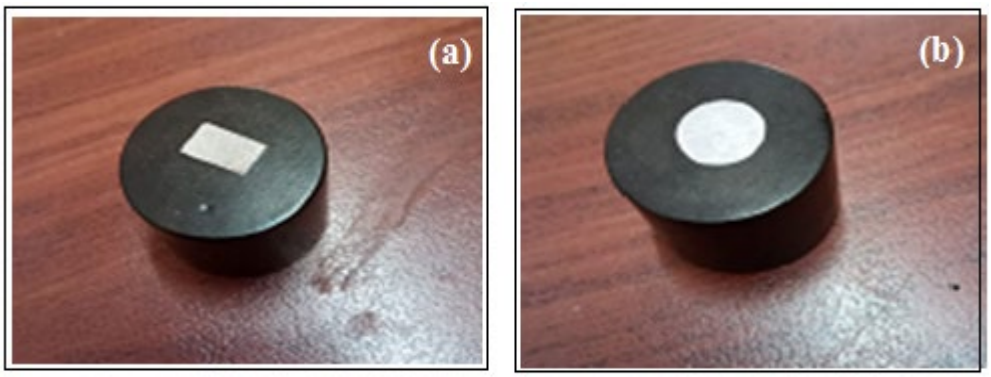

Figure 4. Mounted samples for microstructure and microhardness (a) AC2 and (b) SF2 alloys

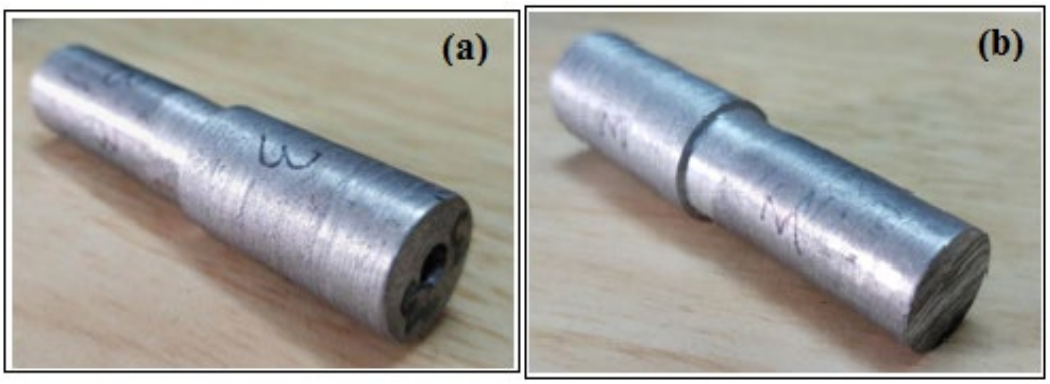

Figure 5. Wear test pins (a) top end (b) wear end

2.3. Wear testing procedure

The cast and spray formed alloys specimen were machined into cylindrical pins of 60 mm × Φ15 mm for conducting dry sliding wear tests (Figure 5) on a pin-on-disc testing machine (DUCOM-Wear & Friction Monitor-TR-20LE) having a steel disk made of of EN-32 material at a sliding velocity of 1.0 m/s (Disc speed- 160 rpm) and varying the normal loads of 10, 20, 30 and 40 N. All the tests were carried out at room temperature and different elevated sliding temperatures (100, 200 and 300ºC) with a wear track diameter of 120 mm and sliding distance of 2000 m and repeated three times. The test pin was heated by inserting the shank portion of the pin into the hole surrounded by a heating element (Figure 6b) and temperature was measured using a commercially available small chrome-alumel type thermocouple foil with a stainless steel sheath of 0.25 mm outer diameter placed inside the hole made at the pin centre. After completion of each wear test at different test conditions, wear samples were cleaned with acetone. Weight loss of pin (ΔW) was calculated by measuring the difference in weight of a pin before and after each test. The wear rate (*WR*) is calculated by using Equation 1.

$$WR = \frac{(\Delta W/\text{density of alloy})}{SD} mm^3/\text{m} \quad (1)$$

Microstructural observation of the worn specimens was studied by using a scanning electron microscope.

Figure 6. (a) Pin-on-Disc testing machine (b) specimen heating attachment.

Figure 7 shows an example of data acquisition (from wear and friction monitor) of the SF2 alloy at 1.0 m/s sliding velocity, temperature of 100ºC and, 50N applied load. It was observed that the initially friction force and COF increased sharply for a sliding time of 400 seconds and then reaching to a steady state regime. The increase in coefficient of friction is due to rough contact surfaces between the pin sample and the steel disc. The ploughing action of hard primary Si and intermetallic asperities on soft aluminium alloy surfaces contributes significantly to the higher friction force and COF during the initial sliding period. Once an ideal contact is reached, the COF or friction force shows steadt state value [24] .Moreover, it can be seen that the temperature at the interface changes between 1 and 5 °C.

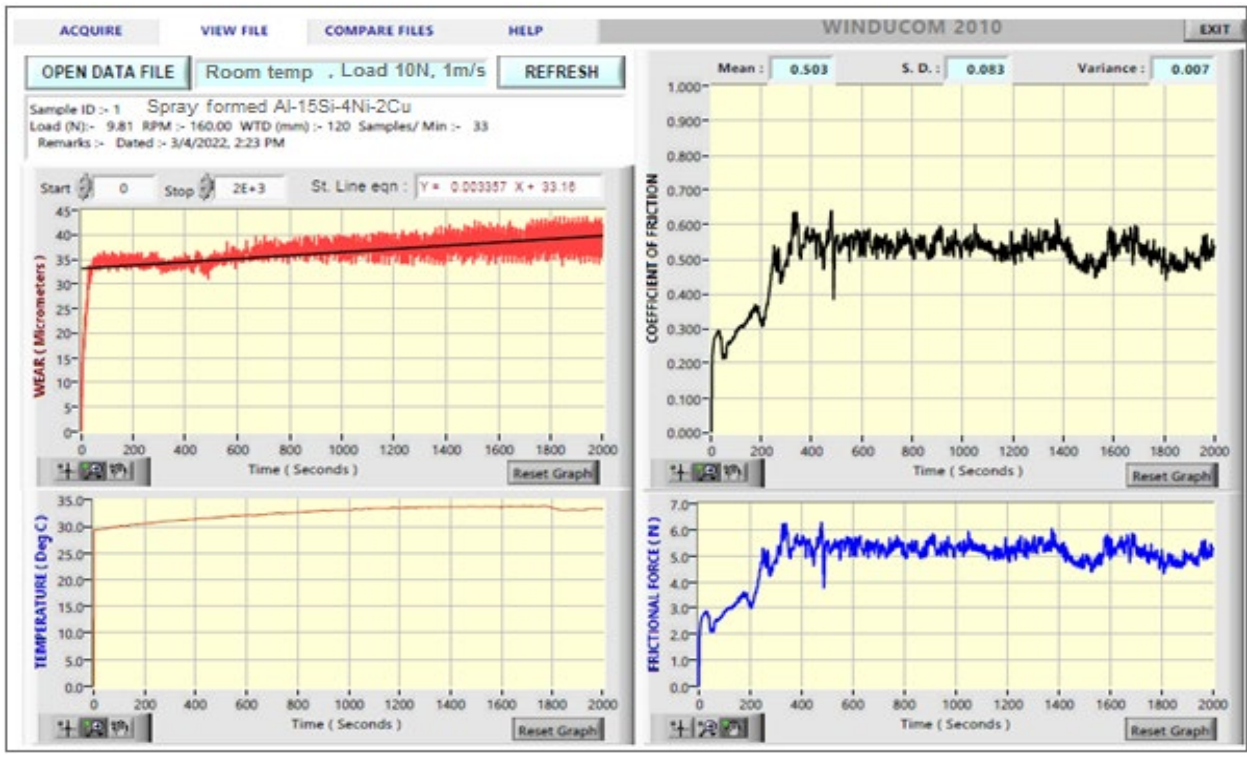

Figure 7. Example data acquisition plot at room temperature during dry sliding wear of SF2 alloy at 10N load, and 1.0 m/s sliding velocity

3. Results and Discussion

3.1. Microstructure

Figure 8(a) shows optical microscopic image of the AC1 alloy, which consists of long needle/acicular form of eutectic Si, and coarse blocks with sharp-edged primary Si particles non uniformly dispersed in the dendrite Al matrix. The AC2 alloy (Figure 8b) consists of primary coarse Si, a flake/acicular eutectic phase, Cu rich intermetallic in block-like form and a network of the short strip, and the reticular form of Ni-rich intermetallic phases in the inter-dendrite regions of the matrix. The primary Si particles having a size of 75±5 µm exist in the form of block with sharp edges. A similar observation was also reported by Camarillo-Cisneros et al

[25]. The microstructure of Al-15Si (SF1) alloy (Figure 8c) consists of fine, spherical primary Si and eutectic Si phases evenly distributed throughout the Al matrix. The optical micrograph of the Al-15Si-4Ni-2Cu (SF2) alloy (Figure 8d) shows the presence of fine, spherical primary Si and eutectic Si phases and fine Ni-rich and Cu-rich intermetallic particles uniformly dispersed in the equiaxed Al matrix. Primary Si particles are 25 ± 1.7μm in size and have an aspect ratio of 1.5 ± 0.26 and intermetallic particle sizes are 10 ± 1.2 μm with an aspect ratio of 7±1.3.

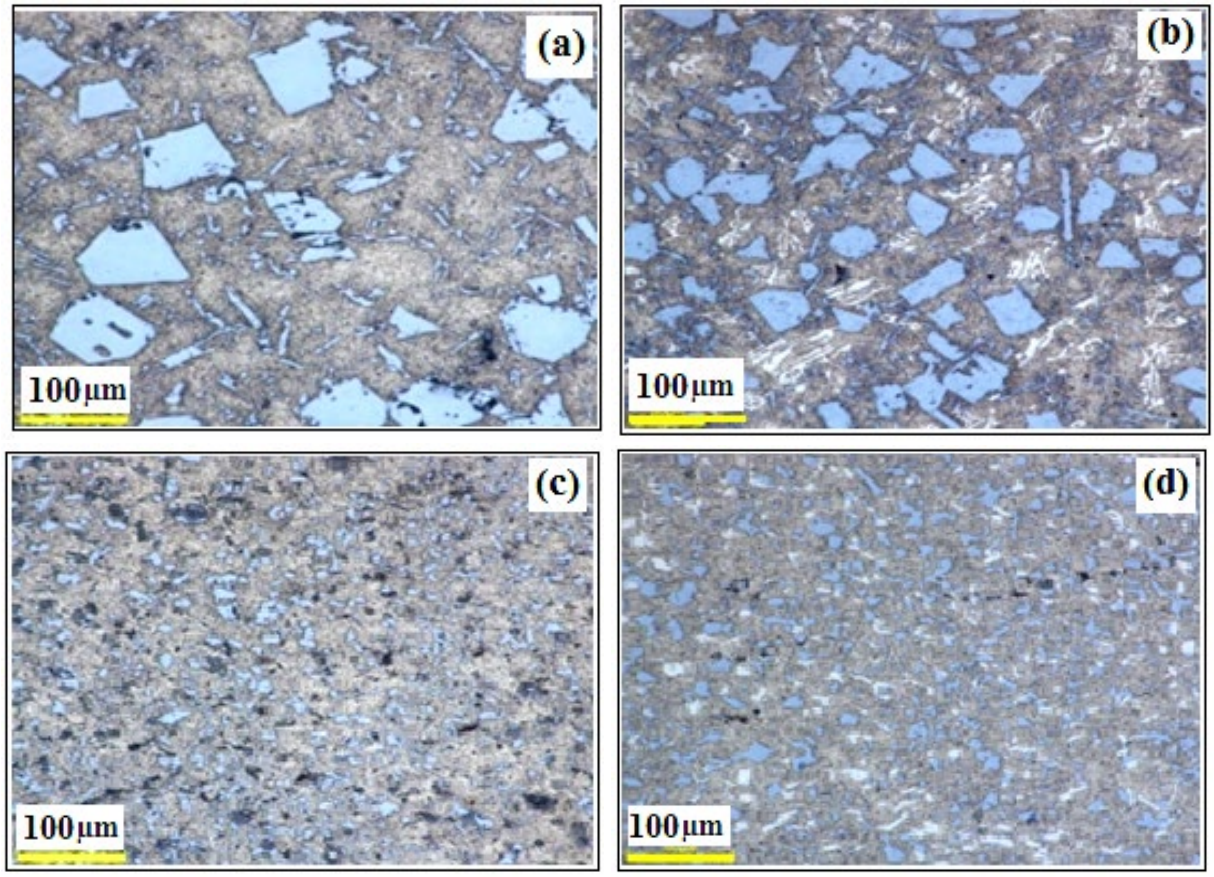

Figure 8. Optical microstructures of (a) AC1, (b) AC2, (c) SF1 and (d) SF2 alloys

Figure 9 shows the SEM/EDS microstructures of the AC1 alloy. It mainly consists of α-Al dendrites, eutectic and primary phases. The primary Si phase exists in black color in the form of a coarse block, the eutectic Si phase which is in (dark gray color) a long needle and light gray is the α dendritic Al- matrix.

The chemical compositions of the phases are presented in Table 3. Figure 10 shows the SEM micrograph of the AC2 alloy. It consists of a coarse primary Si phase, eutectic Si, Cu- rich and Ni-rich intermetallic phases and a dendrite structure of Al matrix. From the EDS spectra (Figure 10b), the white phase (Spot 1) is identified as θ-Al_2Cu intermetallics presented in the form of Chinese script, whereas, the dark grey phase is identified as primary Si. Additionally, presence of Ni (Spot 5) detected as ε-A_3Ni phase (white phase) exist in the form of reticular/needle. The chemical compositions of the phases are shown in Table 4.

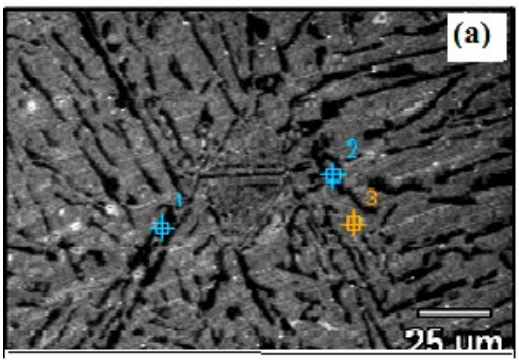

Figure 9. SEM/EDS microstructure of AC1 alloy

Table 3. EDS chemical composition of the phases in AC1 alloy (Figure 9)

AC1 alloy	Elements (wt.%)				
	O-K	*Mg-K*	*Al-K*	*Si-K*	*Fe-K*
EDS Spot-1	0.14	0.08	50.37	49.10	0.30
EDS Spot-2	0.37	0.11	13.76	85.65	0.00
EDS Spot-3	0.46	0.13	98.56	0.37	0.39

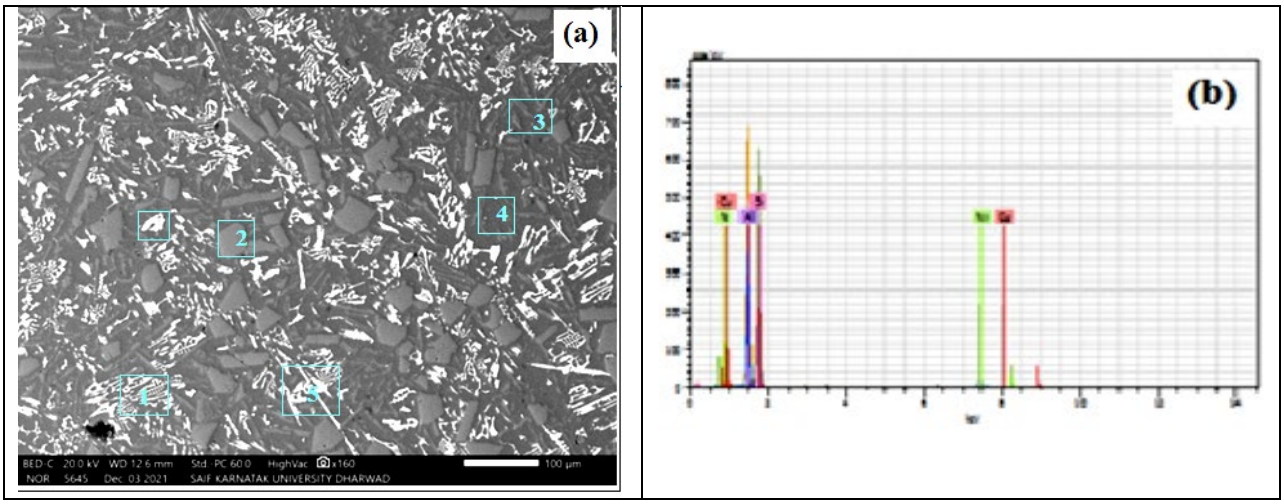

Figure 10. (a) SEM micrograph and (b) EDS spectra of AC2 alloy

Table 4. Chemical composition of the phases by EDS analysis

AC2 alloy	Elements (wt.%)			
	Al	Si	Ni	Cu
EDS spot 1	45.35	0.73	1.56	54.36
EDS spot 2	1.85	97.54	0.33	0.28
EDS spot 3	44.18	53.42	0.41	1.99
EDS spot 4	97.97	1.16	0.24	0.63
EDS spot 5	67.43	0.66	29.52	2.39

The microstructure of the spray-formed alloys is shown in Figure 11. The microstructure of SF1 (Figure11a) consists of primary and eutectic phases in the form of fine and spherical distributed

uniformly in the matrix. The SEM microstructure of the SF2 alloy as shown in Figure 11(b) and the EDS spectra taken (Figure 11c) at various spots indicated in the Figure7(b). The EDS of the SF2 alloy clearly shows the Ni rich white phases (Spot 2 and Spot 3). The dark black phase (Spot 1) mainly consists of primary Si. Additionally, Cu rich phase (Spot 5) presence is also observed. The primary Si and eutectic phases are in the form of fine and spherical particles. The Ni rich and Cu rich intermetallic phases appear in the form of a fine worm structure and are evenly distributed in the equiaxed Al matrix. The chemical composition of the phases presence in the SF2 alloy is shown in Table 5.

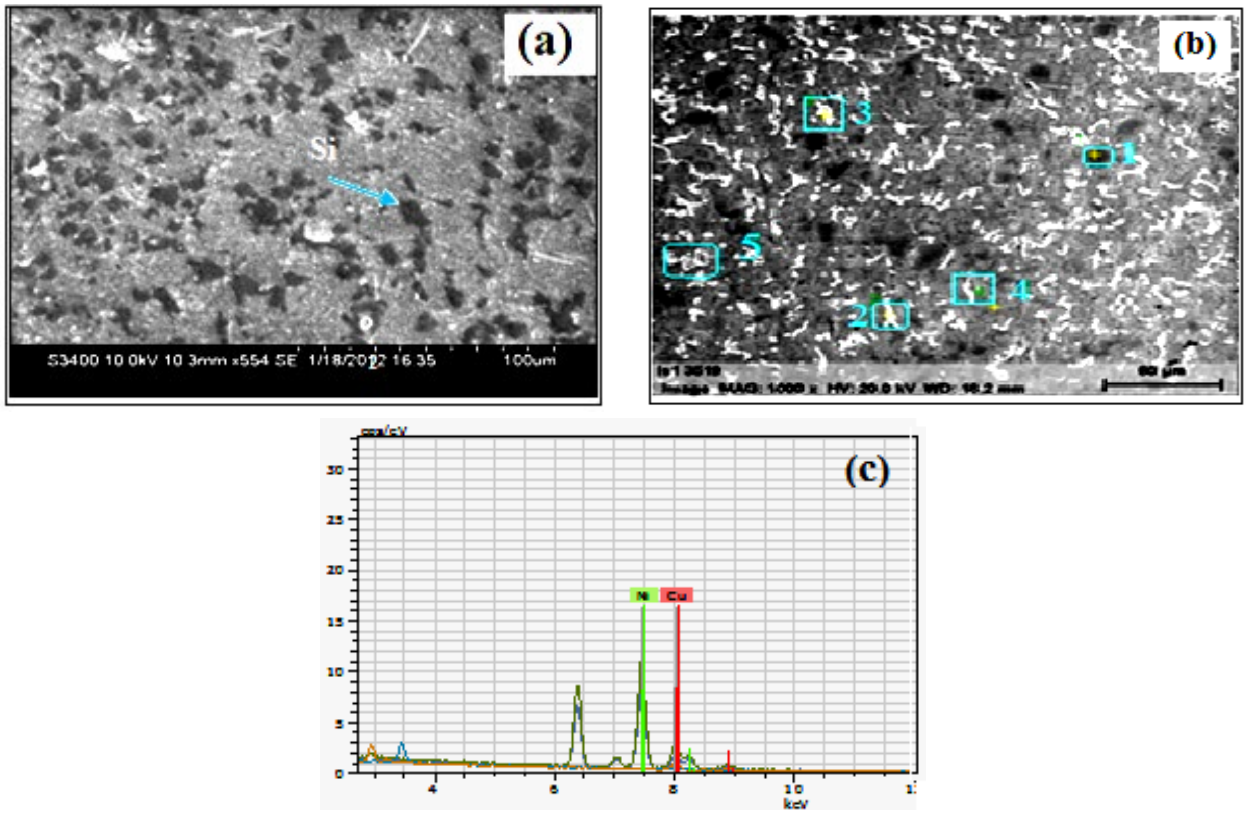

Figure 11. SEM micrographs of (a) SF1, (b) SF2 alloys and (c) EDS spectra of SF2 alloy

Table 5. Chemical composition of phases of the SF2 alloy by EDS analysis

Spot	Phase	Elements (wt.%)			
		Al	Si	Ni	Cu
EDS spot 1	Si	1.28	98.3	0.18	0.24
EDS spot 2	$AlNi_{16}SiCu_{1.2}(\delta)$	64.13	2.14	24.94	8.79
EDS spot 3	Al_3Ni (ε)	74.23	1.11	24.83	1.82
EDS spot 4	Eutectic Si	81.41	17.05	0.16	1.38
EDS spot 5	$Al_{96}Cu_{48}$	54.23	1.23	0.13	44.41

3.2. Hardness

Figure 12 shows hardness values of the cast and spray-formed alloys. It is observed that the spray formed alloys have higher hardness values compared to the cast alloys. The AC2 has a hardness that is almost 12% higher than the AC1 alloy, while the sprayed alloys SF1 and SF2 have hardness values that are almost 36% and 40% higher than the corresponding cast alloys. The results show that the SF2 alloy has a hardness that is almost 24% higher than the SF1 alloy. The presence of fine primary Si, eutectic phase and fine hard intermetallic phases (θ and ε) in the equiaxed Al matrix with increased solid solubility in the spray formed alloys is associated with improvement in hardness. The high hardness of spray formed alloys produced alloys by spray forming due to the presence of fine primary Si, intermetallic θ, ε and eutectic Si phases, possses a significant obstacle to indentation-induced plastic deformation.

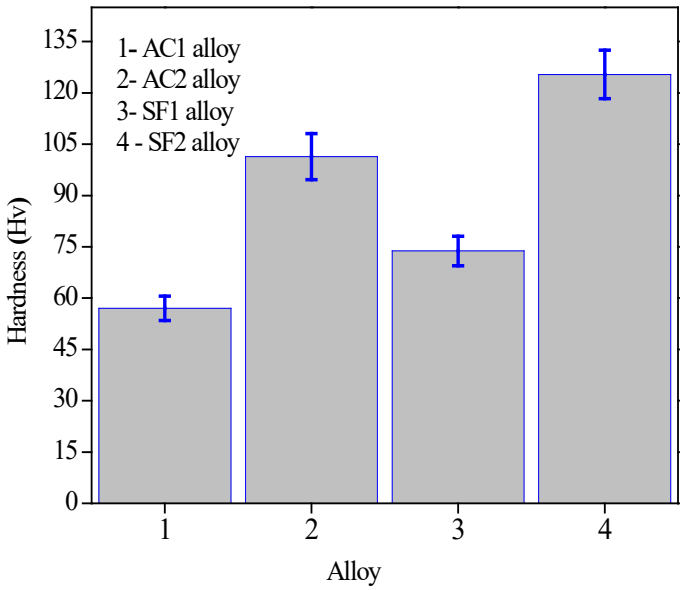

Figure 12. Micro hardness of the cast and spray-formed alloys.

3.3. Wear rate

Figure 13 illustrates the wear rate variation of the cast and spray-formed alloys at different sliding temperatures. It is observed that the wear rate of both the cast and spray-formed alloys increases linearly with the increasing applied load for different sliding temperatures which vary from room temperature (RT) to 300ºC. The wear rates at RT for the AC1 and AC2 alloys are higher compared to the SF1 and SF2 for the entire applied load range from 10 to 50 N. The alloy composition had a significant impact on the wear rate. Compared to AC1, AC2 alloy has a lower wear rate. However, the SF2 alloy shows the lowest wear rate in the whole applied load range and sliding temperature between RT and 300ºC. It is observed that there is a remarkable difference in wear rate between AC1 and AC2, especially at higher loads.

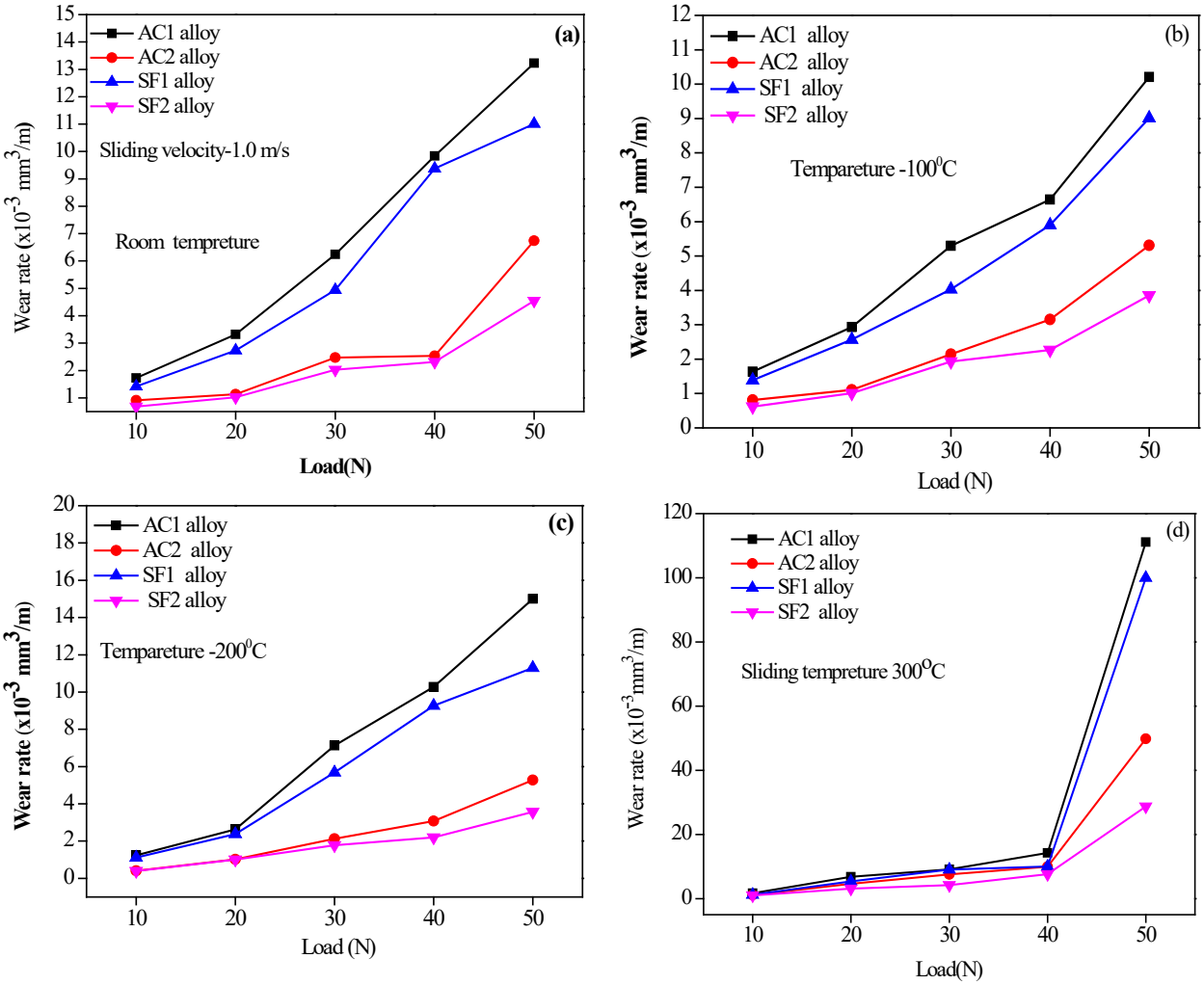

Figure 13. Variation of wear rate with load at temperatures of (a) 30°C,(b)100°C, (c) 200°C and (d) 300°C.

The increasing trend of the wear rate with increasing applied load causes an increase in the sliding contact area and excessive plastic deformation of the asperities, resulting in a greater degree of wear particle generation and a higher wear rate. The results show that the wear rate of the SF2 alloy is approximately 61%, 57%, 52%, and 42% lower than that of the SF1 alloy at RT, 100, 200, and 300°C sliding temperatures respectively over the entire applied load range. This can be attributed to the microstructural modifications in the SF2 alloy. The relatively high hardness of the SF2 alloy and the resistance provided by the fine and evenly distributed primary Si, Al_2Cu and Al_3Ni particles in the Al matrix. The fine, hard particles are less prone to micro cracks; in other words, the smaller the particles, the less likely they are to rupture. The ability of the matrix to accommodate the Si and intermetallic particles improves as the service temperature increases within limits due to the better ductility properties of the matrix.

The high wear rate in the AC1 and AC2 alloys could be due to the presence of large irregular coarse Si particles, hard coarse intermetallic and needle-like eutectic Si with a high aspect ratio, resulting in high stress concentrations at the particle/matrix interface and an easy pathway for

crack initiation and propagation [26]. The interaction of these cracks leads to the detachment of planar wear particles through the delamination wear process. In addition, Si particles with higher aspect ratios are more prone to fragmentation. Due to the deboning between particle and matrix, fragmented Si and intermetallic particles can no longer bear the load so; the disc surface and soft Al matrix come into direct contact. Large stresses are generated in the Al matrix around the contact surfaces, which promotes the development of subsurface cracks and delamination. However, the fragmented, hard Si and intermetallic particles can act as the the third body abrasives and increase the deterioration of the worn surface through an abrasive wear mechanism, resulting in a higher wear rate. Compared to the cast alloys, spray-formed alloys show higher wear resistance both at RT and at elevated interface temperatures. The SF2 alloy exhibits high wear resistance over the full range of applied loads and sliding temperatures. A higher hardness of the spray formed alloys, caused by precipitation and solid solution hardening together with a fine morphology of the intermetallic and Si particles, resulted in a mechanically more stable matrix supporting the formed tribolayer, which increases the wear resistance of the spray formed alloys. The high content of Si and intermetallic compounds leads to a great improvement in wear resistance due to its high hardness, which not only resists plastic deformation and delamination, but also causes oxidative wear, in which an oxide film could improve wear resistance.

The trend also shows that the rate of wear decreases by increasing the temperature levels between RT and 200 °C, which is due to the higher interface temperature leading to the extent of oxidation of the alloys. The thicker glazed oxide layer acts as a wear protection layer, thereby reducing the wear rate. The increase in temperature at the contacts of the interface asperities due to the temperature rise and their interactions enhance the rupture and fragmentation of the mechanically mixed tribolayer. The following were the causes of the higher wear rate with temperature increases above 300^{o}C (critical temperature): (1) As a result of the higher temperature, the material became softer, leading to more abrasive wear. (2) The development of the adhesive bond, the cold welding process at the asperities, and its removal process were all accelerated with an increase in temperature, leading to higher wear by adhesion. (3). Thermal stresses caused by the difference in thermal expansion coefficient became noticeably more intense at higher temperatures, weakening the particle/matrix contact and promoting particle extraction [27].

The intensity of temperature, velocity and their interactions were reduced by increasing the applied load. In sliding contact, friction causes the maximum contact stress to be transferred to the surface. At low loads (i.e 10N-20N) the maximum shear stress is at the subsurface and the

wear rate is controlled by fracture of the oxide layer, removal of oxide debris particles and there is no subsurface deformation at low loads. When the load increases (20-30N), the local stresses generated under the slider are less than the breaking strength of the Si particles. Therefore, the unbroken Si and the intermetallic particles act as the load bearing elements and scratch the surface of the counterpart. Consequently, the aluminum matrix is prevented from being directly involved in wear. However, some particles chipping from the Si and/or other intermetallic particles will wear away the soft aluminum matrix, resulting in a low wear rate. When the load is high (30N-40N), Si and intermetallic particles cannot bear the load. As a result, the Al matrix is directly involved in the wear process due to direct contact with the counter surface. Therefore, a large amount of stress is generated with the Al matrix adjacent to the contact area. This leads to the generation of micro cracks and the propagation of the cracks. In addition, the Si and intermetallic particles break and become wear bodies of the third body, which are responsible for the initiation of the groove profile on the worn surface.

SF1 and SF2 have much lower wear rates than cast alloys at RT and increased temperature for all applied loads, which is particularly important to note. The following factors contribute to the low wear rate of the spray-formed alloys.

(1) High resistance to abrasive wear is offered by the high hardness of spray-formed alloys

(2) The spherical morphology of Si and intermetallic particles caused a reduction in particle/matrix contact area, which in turn reduced the potential for particle pullout in the spray-formed alloy.

(3) The homogeneous distribution of the intermetallic Si, ε and θ particles increases the resistance of the spray-produced alloys to adhesive wear.

(4) The matrix surface, on the other hand, is less exposed to the counter disk and thus, has a lower wear rate.

The fine and hard Si and ε intermetallic particles in the spray formed alloys were more difficult to remove from the surface due to their superior mechanical properties. On the other hand, the abrasion of the rotating disk was caused by the rubbing action of hard Si and intermetallic particles. As a result, iron oxide debris was generated and mixed with alloy debris. Fresh oxides developed on the wear marks, which were subsequently removed by the pin as it wore. As a result of the continued attrition of this debris, which sintered under the applied force, a tribolayer, or mechanically mixed layer, developed. According to reports, the presence of such a layer significantly reduces wear [28]. In addition, the thermal stability of the spray-formed alloys

was better than that of the cast alloys due to the uniform distribution of the thermally stable Ni-rich phases and Al_2Cu particles.

Specific wear rate is defined as the wear rate per unit applied load. Figure 14 shows the variation in specific wear rate of the cast and spray-formed alloys as a function of applied load and temperatures at a sliding speed of 1.0 m/s. In the RT condition (Figure 14a), it is observed that the specific wear rate gradually decreases for both cast and spray formed alloys at loads between 10 and 20 N. This may be because the alloy is work-hardened during the wear test, which increases the load-bearing capacity and thereby imparts improved wear resistance. The pattern of increasing specific wear rate in cast alloys with increasing applied load. However, the specific wear rate in the spray-formed alloys is the same between 20 and 40N loads and gradually increases after the 40N load is applied. The specific wear rate of alloys at temperatures of 100 °C is shown in Figure 14(b). The specific wear rate of the cast alloys has been found to be constant for the applied loads between 10 and 40 N and gradually increases for the load above 40 N. In the case of spray-formed alloys, the specific wear rate is constant and gradually increases as the load increases above 40 N. Figure 14(c) shows the influence of normal loading on the specific wear rate at an interface sliding temperature of 200°C. It was found that the cast alloys show a similar trend of constant specific wear rate at applied loads between 10N and 20N, and at high loads above 20N, the specific wear rate increases significantly. For spray-formed alloys, the specific wear rate increases steadily with increasing load. At the sliding temperature of 300ºC (Figure14d), the specific wear rate of both cast and spray formed alloys remains constant between an applied load of 10 to 40 N and increases rapidly with the increasing applied load. It is clearly observed that, in the entire applied load range between 10 to 50N and interface temperature from RT to 300ºC, the cast alloys show significantly higher specific wear rate than that of spray formed alloys respectively and the SF2 alloy depicts less specific wear rate compared to the SF1 alloy. The values of cast alloys (AC1 and AC2) in the entire applied loads from 10 to 50 N and temperature between RT and 200ºC, are between 1.32×10^{-4} mm^3/Nm and 3×10^{-4} mm^3/Nm and. However, at 300ºC sliding temperature, the values of AC1 and AC2 alloys show 1×10^{-4} at load between 10 to 42 N and beyond which, the values are in the order of 1×10^{-3} mm^3/Nm. The specific wear rate values of the spray-formed alloys (SF1 and SF2) are in the order 10^{-5} to 10^{-4}. According to [29], the specific wear rate ranges from 10^{-7} to 10^{-4} mm^3/Nm, in this case, the state of wear is known as "mild wear" defined by a small wear rate caused by oxidative wear, and the specific wear rate in the range of 10^{-3} mm^3/Nm, indicating that the wear in these alloys is in the severe wear mode and caused either by abrasive and adhesive or combined abrasive and adhesive modes of wear. When the specific wear rate is less than 10^{-5} mm^3/Nm, the wear mode termed as "oxidative wear," which is connected to tribo-chemical wear,

forms metal oxide-based wear particles [30]. The formation of a stable oxide layer between the mating surface and the pin material, which was stable enough to withstand the load, was attributed to the low specific wear rate at the low loads. At the higher loads, the temperature differences between the mating surface and the pin material embrittles part of the oxide film layer, resulting in an increased specific wear rate. The oxide layer was initially quite thin and spread out as a thick layer as the sliding distance increased. Due to the work hardening effect, the oxide layer started cutting the surface of the pin since it was harder than the pin material. As a result, the worn surface consisted of multiple ridges and elongated grooves extending parallel to the sliding direction. The abrasion wear mechanism was found to be responsible for this.

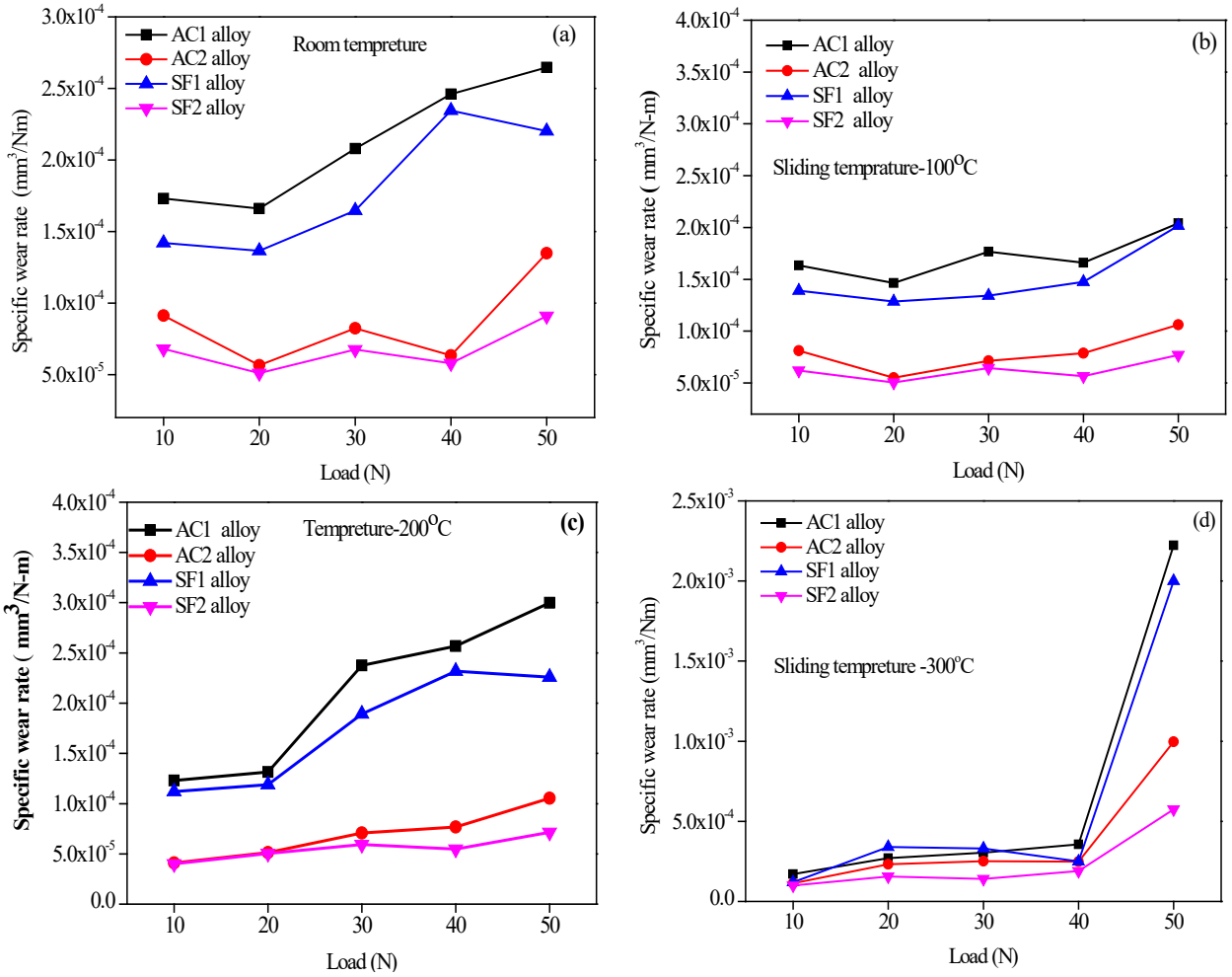

Figure 14. Variation of specific wear rates with load at (a) room temperature (b) 100°C, (c) 200°C and (c) 300°C

Rise in sliding temperature from RT to 200°C, the wear rate is not significant with the increasing load from 10 to 50N. At low load, in response to the thermo- mechanical loads, oxide typically forms as thin surface layers with a thickness that ranges from a few to hundreds of nanometers to prevent direct metal-to-metal contact and reduce friction by limiting any adhesive wear. The two main types of wear that are known to occur often are abrasion and adhesion, and the severity of both of these mechanisms is typically exacerbated at high temperatures. Abrasion happens when

sharp edges on a hard surface and/or hard particles in the contact area are cut into softer materials. At high temperatures, the thermal softening of the matrix and the presence of hard, oxidized wear particles encourage abrasion. On the other hand, extreme adhesion, or galling, forms as a result of the bonding of the materials in contact and the following material transfer from one surface to another [31]. High sliding temperatures cause the oxide layers to shatter more easily, expose reactive metallic aluminum alloy, and increase the true contact area, all of which accelerate the adhesive wear. The softening of the contacting material as a result of high interface temperatures affects bulk mechanical properties such as yield strength, hardness, and toughness. This reduces the mechanical support of the surface layers (surface oxides) [32]. As a result, material plastic deformation and surface layer delamination can occur.

2.4. Coefficient of friction

The ratio of frictional force to applied load between two surfaces is quantified as the coefficient of friction (COF). It is a measure of the friction behavior of the material. Figure 15 shows the change in COF as a function of the applied loads and temperatures. It is observed that the COF showed a decreasing trend with increasing load for both the cast and spray formed alloys. It is also evident from the results that the average coefficient of friction is lowest for both AC2 and SF2 at temperatures between RT and 100°C and the higher value of COF was recorded at a sliding temperature of 200 and 300°C. The results show that the COF of spray-formed alloys are lower than those of corresponding cast alloys. The average COF of the SF2 alloy is less than the SF1 alloy. In the cast alloys, the matrix alloy surrounding the coarse primary Si, the hard needle and acicular form of the Cu and Ni rich intermetallic phases is eroded and essentially all contact between the primary (Si and intermetallic) particles is lost and the provided mating surface made of steel.

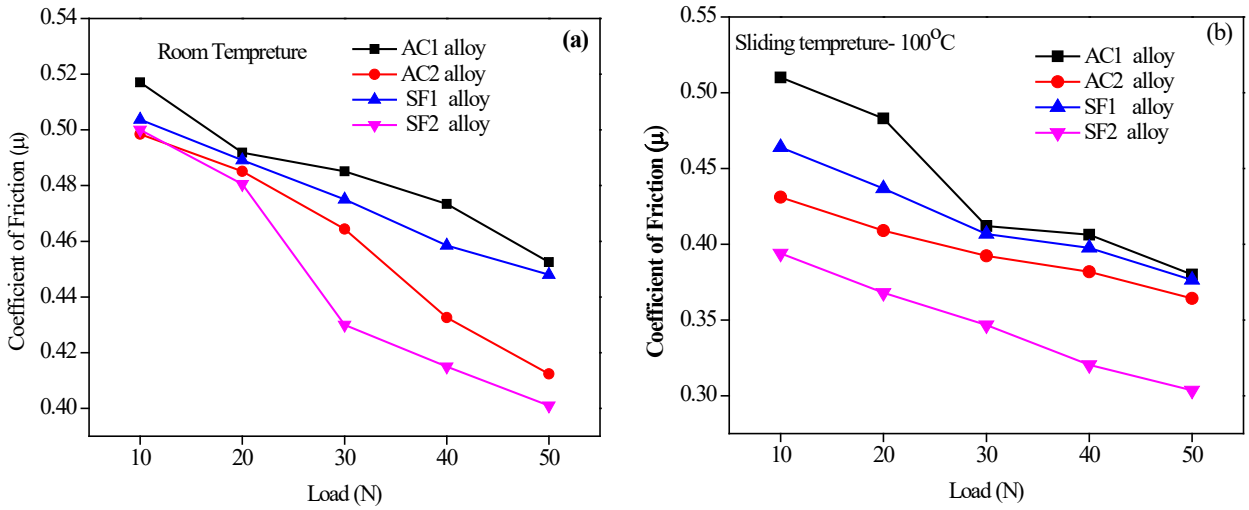

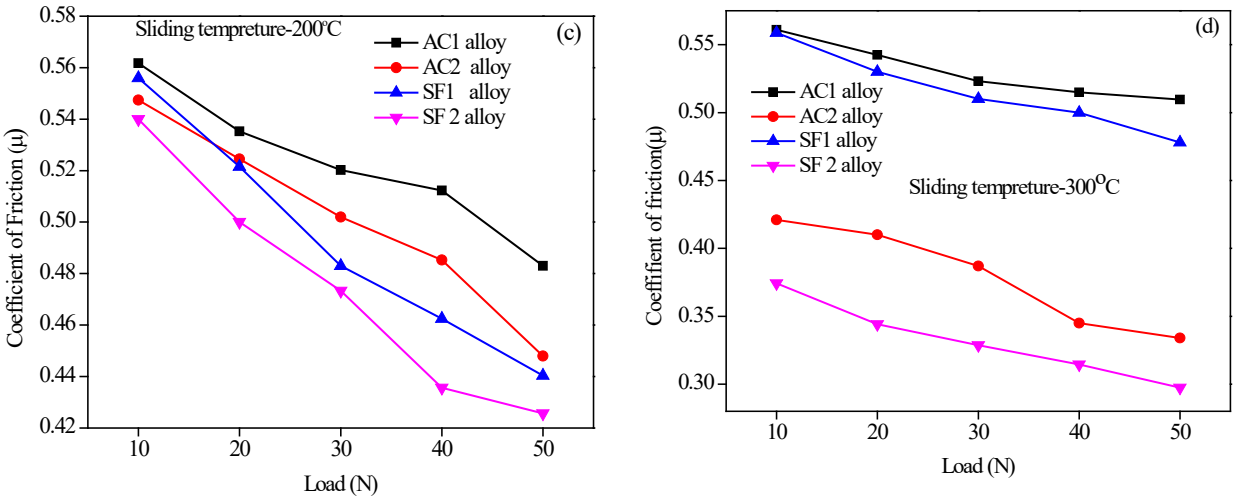

Figure 15. Variation of friction coefficients with applied load at different sliding temperatures (a) room temperature (b) 100°C,(c) 200°C and (d) 300°C.

3.5. Worn surface morphology and wear map

When the particle de-cohesion is very easy, there is direct contact between the matrix and the steel mating surface, and the dissolved hard particles cause third-party abrasion mechanisms, resulting in increased surface roughness between contact surfaces and increased friction coefficient [33]. The wear rate is largely controlled by the rate at which particles delaminate from the matrix. Similarly, this can be clearly seen at the RT and 200°C test temperatures. The rate of wear is largely controlled by the rate at which particles detach from the matrix. Similarly, this can be clearly seen at the test temperatures of RT and 200°C. The coefficients of friction were low, showing similar values between samples up to a transition temperature of 200°C and increasing rapidly with increasing temperatures above 200°C, which is a transient wear phenomenon believed to be mainly due to the transition from mild wear to severe wear.

The morphological features of worn surfaces of both cast and spray formed alloys were studied at a sliding speed of 1.0 m/s and a load of 50 N at different sliding temperatures to identify wear mechanisms. The SEM micrographs of the worn surface of the casting and the spray formed samples sliding at RT are shown in Figure 16. The worn surface of AC1 alloy (Figure 16a) is characterized by deep and wide grooves running from end to end of the surface. It also consists of microgrooves, craters and grinding marks. Some large pits are also seen, suggesting that block type primary Si phases have fractured and broken off during wear. The AC2surface (Figure 16b) shows long, continuous parallel grooves, large, shallow, compacted oxide patches, discontinuous abrasive grooves, and surface cavities. Some large dimples can also be seen, which indicates that block-like primary Si and intermetallic phases are fractured and broken off during wear. Abrasive wear occurs when hard Si particles are introduced between the two sliding surfaces. The grooves and dimples are shallower than in the AC1 alloy. Surface damage is seen in this

alloy also, but the intensity of the damage is less as compared to that of the AC1 alloy. The worn surfaces of spray-formed (Figure 16c-d) consist of a smooth wear surface including fewer craters and smoother tribological oxide layers. The worn surface also exhibits a small number of small dimples and a very small number of scoring marks extending from one end to the other. Additionally, the surface reveals the presence of white patches, which at this stage are a sign of oxide formation. The improved volume fraction, size and shape of Al_2Cu and Al_3Ni intermetallic phases and Si particles could reduce stress concentration and improve wear resistance of spray formed alloys by retarding subsurface crack initiation and propagation.

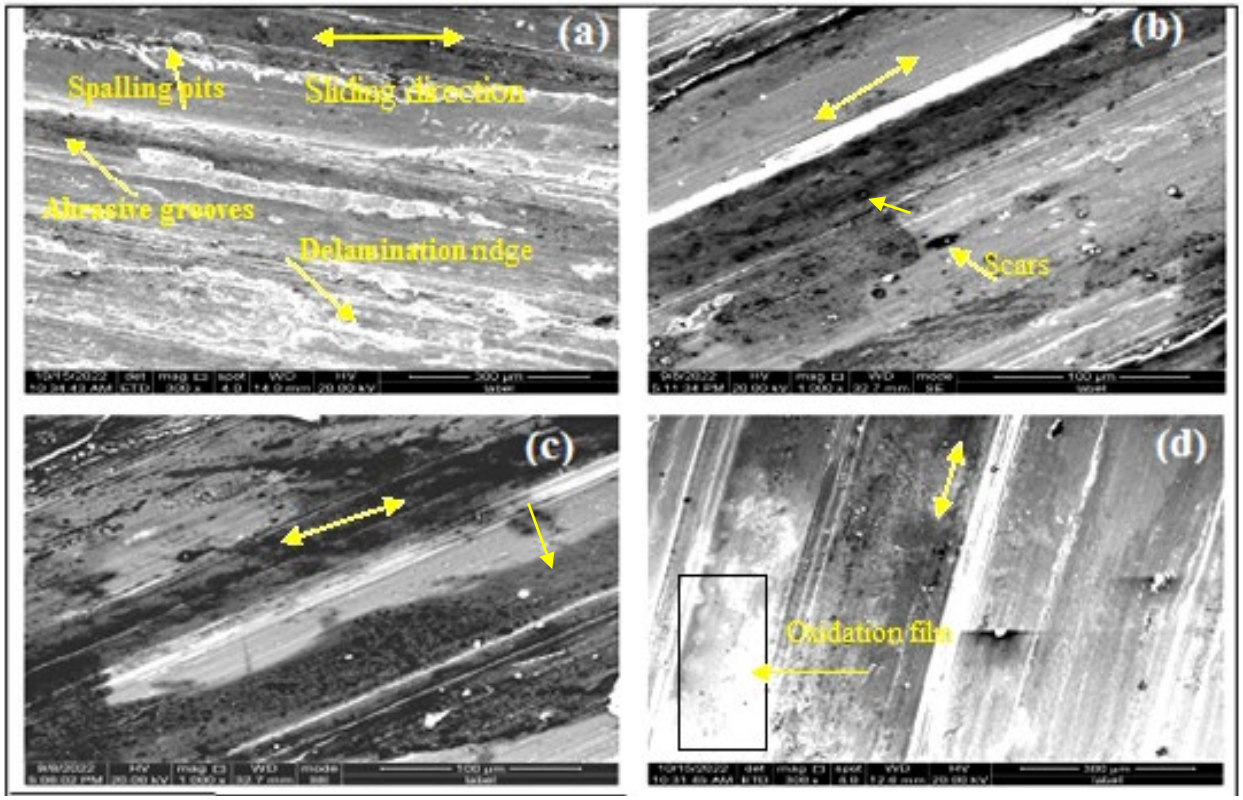

Figure 16. SEM micrographs of worn surfaces of cast and spray formed alloys sliding at room temperature and a sliding velocity of 1.0 m/s under a load of 50N: (a) AC1, (b) AC2, (c) SF1 and (d) SF2.

Figure 17 shows the SEM images of worn surfaces the AC1 alloy tested at 100°C. (Fig. 17a) It consists of fine, smooth-edged grooves that are prominent with small indentations on the surfaces and patches of oxide layers. The worn surface of AC2 is (Figure 17b) characterized by a relatively smooth surface with fine ridges and plowing marks. In addition, a limited number of small pits and very few ridges extending from end to end and the presence of white spots indicating oxidation wear and the formation of continuous wear grooves and some damaged areas and plowing marks indicate abrasive wear. In comparison to the wear surface of cast samples, the worn surfaces of spray produced (SF1 and SF2) alloys (figures 17 c-d) alloys

consist of shallow and smooth and the wear surface morphology has smaller craters and smoother tribological oxide layers.

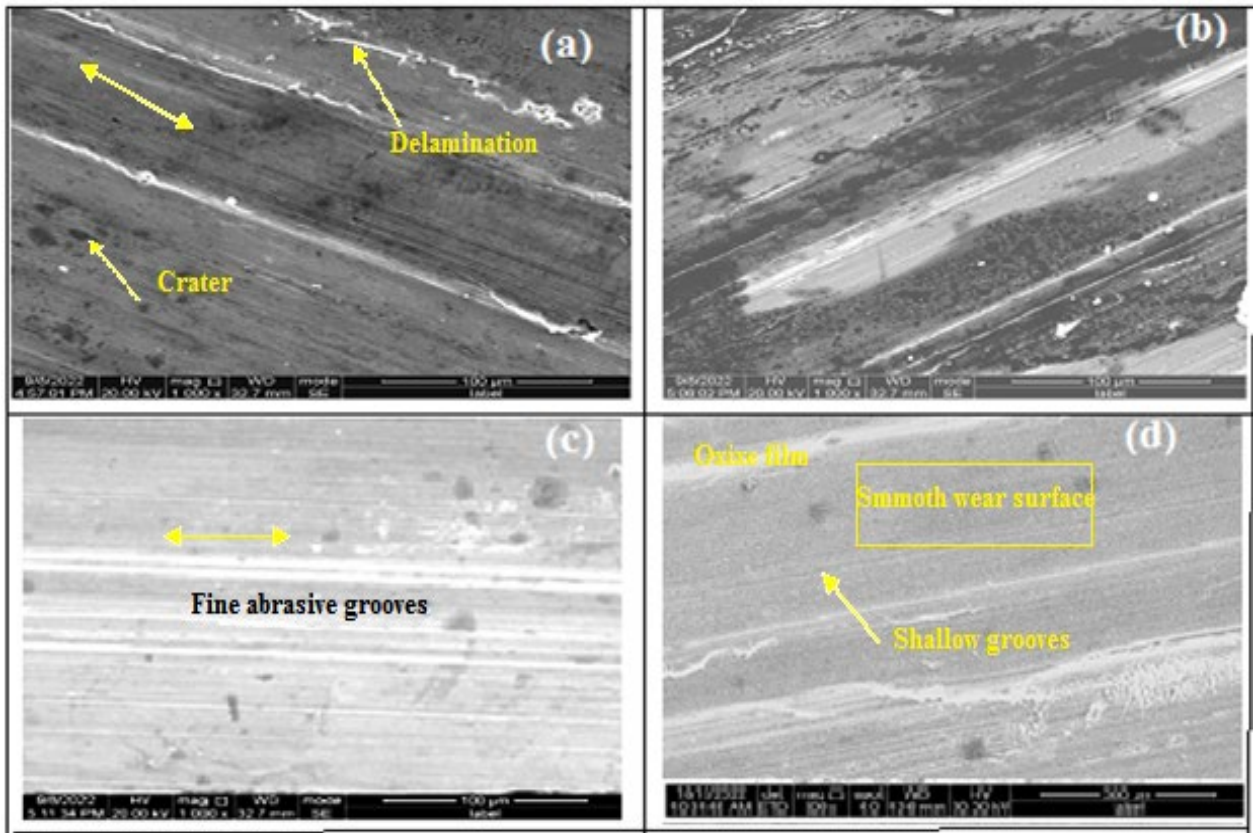

Figure 17. SEM micrographs of worn surfaces of the alloys sliding at 100ºC for a fixed sliding velocity of 1.0 m/s under a load of 50N: (a) AC1, (b) AC2 , (c) SF1 and (d) SF2.

Figure 18 depicts the SEM worn surfaces of the cast and spray-formed alloys at a sliding temperature of 200°C. The worn surfaces of AC1 and AC2 (Figure18a-b) alloys are distinguished by small irregular scars and scratch marks that are parallel to the sliding direction. It also has fine grooves and plowing marks that indicate abrasive wear. In addition, a series of scale-like ridges along with delamination scars and the presence of delamination patches on all worn sample surfaces may indicate the presence of an adhesive wear mechanism. The worn surface of spray formed alloys is shown in Figure 18(c-d). It is clearly seen that the worn surface shows a smooth surface of very shallow and narrow microgroove. In addition, limited number of small dimples and very few scoring marks extending from one end to the other can be seen on the worn surface. The surface also shows the presence of white patches and spots which are indicative of oxide formation. Therefore, the wear surface features shown are typical of abrasive wear, where the asperities of the hard surface dig into the softer material and the material removal is mainly by plowing, resulting in the formation of grooves on the wear surface.

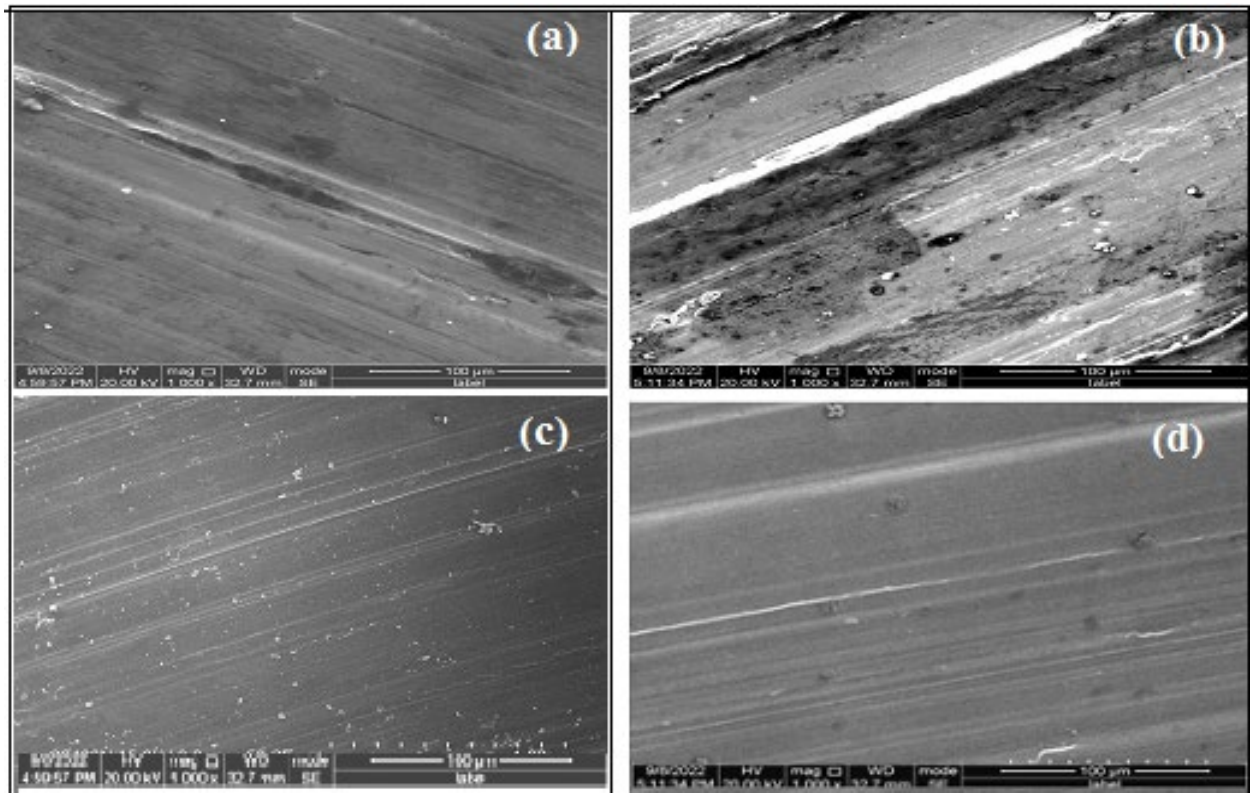

Figure 18. SEM micrographs of worn surfaces of the alloys sliding at 200ºC for a fixed sliding velocity of 1.0 m/s under a load of 50N: (a) AC1, (b) AC2 , (c) SF1 and (d) SF2.

The worn surface of the alloys at the sliding temperature of 300ºC is shown in Figure 19. The worn surfaces of the AC1 and AC2 are characterized by heavier material flow along the sliding direction at 300ºC (Figure 19a-b).Typical microstructural characteristics include oxidation of the surface layers and severe lath kinking, which signifies substantial plastic shearing, deformation bands, fragmentation, and particle pullout zones. On the specimen surface, the worn surfaces show wavy material flow and more severe localized adhesion. The edge cracking and metallic fracture of ridges were seen on the surface of AC1 and AC2 materials. Since friction between the two mating surfaces causes adhesive wear, the two surfaces in contact will be more likely to transfer materials [34]. The worn surface of the sprayed alloys (Figure 19c-d) shows a smooth appearance and markings with minor ridges and a few pits. This can be explained by the fact of oxidation of asperities and delamination on the surface. The formation of oxide is referred to as a "mechanically mixed layer," which acts as a solid lubricant in reducing the wear rate. Oxidation wear should be caused by an increase in temperature. At higher temperatures, further oxidation, densification, and sintering can lead to the development of hard oxide glaze surfaces on these layers, resulting in lower wear rates. The worn surfaces of the spray-formed alloys also showed improved wear surface morphology, such as smaller craters and smoother tribological oxide layers [35-36].

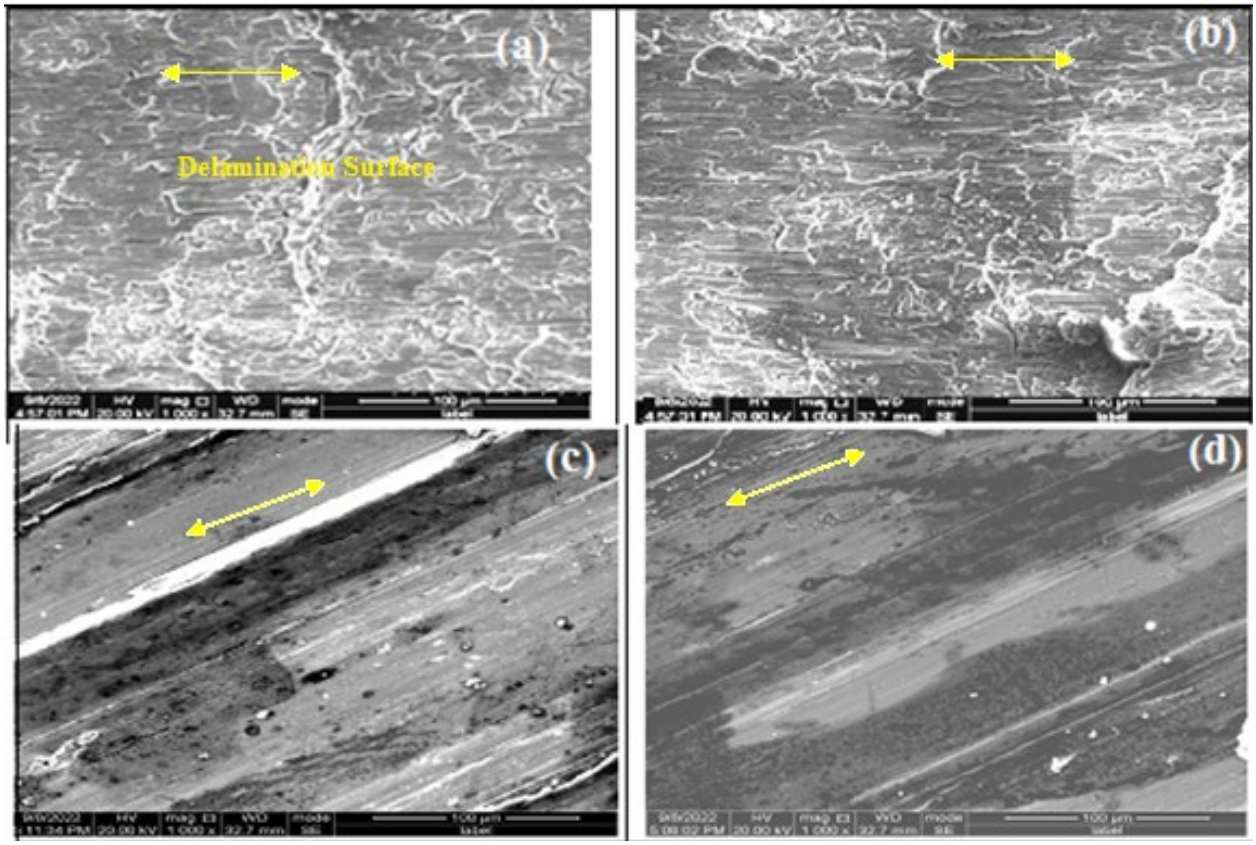

Figure 19. SEM micrographs of worn surfaces of the alloys sliding at 300ºC for a fixed sliding velocity of 1.0 m/s under a load of 50N: (a) AC1alloy, (b) AC2 alloy, (c) SF1 and (d) SF2.

Wear maps can be used to analyze material wear as a function of sliding speed, load, temperature and link-related material removal mechanisms. Wear regime maps provide useful information about changing the wear rates. Figure 20 shows the wear mechanism transition maps displayed on the load-temperature reference frame at a constant sliding speed of 1.0 m/s. A wear map for cast and spray-formed alloys was derived from experimental data and microscopic examination of worn surfaces. Different wear mechanisms, including oxidative, abrasive, adhesive, and severe plastic deformation, combined with a combination of different wear mechanisms, caused the alloys to exhibit very mild, mild, and severe wear rates.

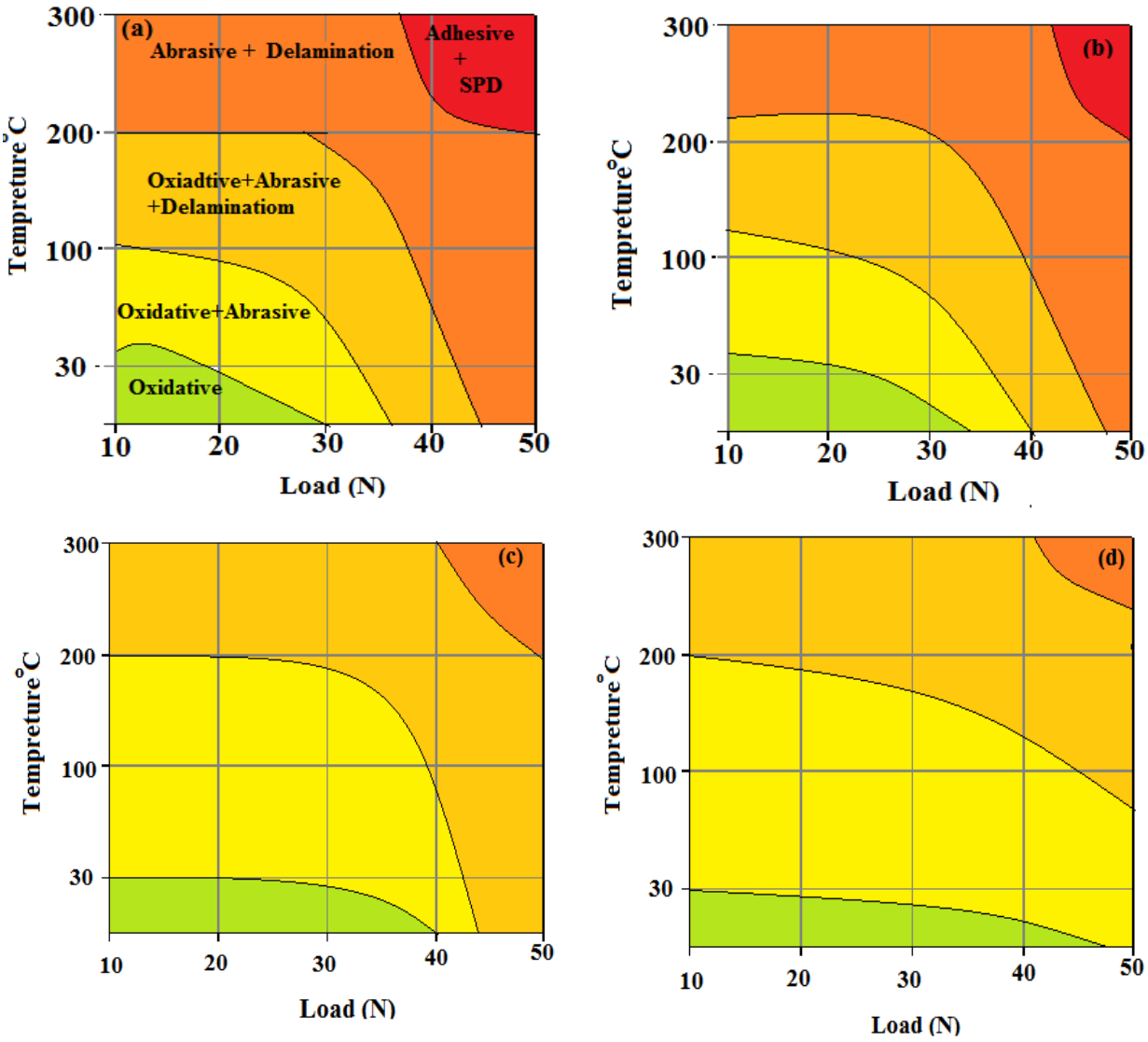

Figure 20. Wear mechanism transition map of the alloys at different sliding temperatures and loads for (a) AC1, (b) AC2, (c) SF1 and (d) SF2 alloys. SPD: severe plastic deformation

4. Conclusions

The spray-forming method combines low-cost manufacturing with enhanced performance and characteristics. The ideal spray-formed microstructure often consists of fine, equiaxed or nearly spherical grains. The spray-formed alloy is ideal for producing with microstructural homogeneity, low levels of micro segregation and the absence of columnar or dendritic morphologies. In the present study, the influence of Ni and Cu addition in hypereutectic spray formed Al-15Si alloy on the tribological properties at elevated temperature was studied. The wear study was carried out at different loads and different temperatures and at a constant sliding velocity of 1.0 m/s. The following are the inferences made from the findings:

The microstructure of the spray formed Al-15Si alloy consists of fine, spherical primary Si and eutectic Si phases evenly distributed throughout the Al matrix. The micrograph of Al-15Si-4Ni-2Cu shows the presence of fine spherical primary Si and eutectic Si phases and fine Ni-rich and

Cu-rich intermetallic particles uniformly dispersed in the equiaxed Al matrix. The cast Al-15Si-4Ni-2Cu alloy consists of primary coarse Si, a flake/acicular eutectic phase, Cu rich intermetallic in Chinese-script/ block-like form and a network of short strip. It has sharp-edged primary Si particles non uniformly dispersion in the dendrite Al matrix.

The spray formed Al-15Si-4Ni-2Cu alloy has a hardness that is almost 24% higher than the spray formed binary alloy. The presence of fine primary Si, the eutectic phase, and hard intermetallic phases in the equiaxed Al matrix, together with higher solid solubility, has improved the hardness of the spray-formed Al-15Si-4Ni-2Cu alloy.

The wear rate of both cast and spray-formed alloys increases linearly with the increasing applied load throughout sliding temperature, which varies from room temperature to 300ºC.

The spray-formed alloys show a lower wear rate in the whole applied load range from 10 to 50N and a sliding temperature between RT and 300°C. The wear rate of the spray formed Al-15Si-4Ni-2Cu alloy is approximately 61%, 57%, 52%, and 42% lower than that of the spray formed Al-15Si alloy at RT, 100, 200, and 300°C sliding temperatures, respectively, and over the entire applied load range

Compared to the cast alloys, spray-formed alloys show higher wear resistance both at RT and at elevated interface temperatures. The Al-15Si-4Ni-2Cu alloy exhibits high wear resistance over the full range of applied loads and sliding temperatures.

The results show that the coefficient of friction of spray-formed alloys is lower than cast alloys.

Authors' contributions: Mehabubsubahani R. Alavandi: Literature search, Methodology, experimental data analysis and drafting. Dayanand M. Goudar: Conceptualization, data curation, review, editing and supervision.

Acknowledgements: The authors would like to thank VGST, Karnataka for supporting the current research.

Funding: Not applicable.

Availability of data and materials: Not applicable.

Declarations

Ethics Approval: Not applicable.

Consent to Participate: Not applicable.

Consent for Publication: Not applicable.

Competing interests: The authors declare no competing interests.

References

1. Qasim. ZM. Jabbar. M. Hassan J(2017)Enhancement the Mechanical Properties of Aluminum Casting Alloys(A356) by Adding Nanorods Structures from Zinc Oxide. J Mater. Sci. Eng 4:1–8.
2. Kaufman JG. Rooy EL(2004) Aluminum Alloy Castings: Properties, Processes, and Applications ISBN: 978-0-87170-803-8 ASM International
3. Alshmri F. Atkinson HV. Hainsworth SV. Haidon C. Lawes SDA(2014) Dry sliding wear of aluminum-high silicon hypereutectic alloys.Wear313(1):106-116.
4. Dongwon Shin. Shibayan Roy. Beta Thoma.R. Watkins. Amit Shyam (2017) Lattice mismatch modeling of aluminum alloys.Computational Materials Science 138:149-159.
5. Erdem KARAKULAK, Muzaffer ZEREN, Ridvan YAMANOĞLU(2012) Effect of heat treatment conditions on microstructure and wear behavior of Al4Cu2Ni2Mg alloy. Trans. Nonferrous Met. Soc. China 23(2013) 1898−1904.
6. William S. Ebhota. Tien-Chien Jen(2018) Intermetallics Formation and Their Effect on Mechanical Properties of Al-Si-X Alloys DOI: 10.5772/intechopen.73188.
7. Sunil.B.Rajeev VR. Jose.S(2017) Dry wear characteristics of nickel rich Al-Si-Cu piston alloys. International Journal of Scientific & Engineering Research8(2)ISSN 2229-5518.
8. Mohammad Salim Kaisera. Sakib Hasan Sabbirb. Mohammad Syfullah Kabirb. Mashiur Rahman Soummob. Maglub Al Nurb (2018). Study of Mechanical and Wear Behavior of Hyper-Eutectic Al-Si Automotive Alloy Through Fe, Ni and Cr Addition Materials Research21(4).1-9.DOI: http://dx.doi.org/10.1590/1980-5373-MR-2017-1096.
9. Yamanoglu.R.Karakulak.E.Zeren.M.Koc.FG(2013) Effect of nickel on microstructure and wear behavior of pure aluminum against steel and alumina counterfaces. International Journal of Cast Metals Research 26(5):289-295.
10. Das.S.Prasad. SV.Ramachandran.TR(1989) Microstructure and wear of cast Al-Si alloy-graphite composites.Wear133:173-187.
11. Yunguo Li. Yang Yang. Yuying Wu Liyan Wang. Xiangfa Liu(2010) Quantitative comparison of three Ni-containing phases to the elevated-temperature properties of Al-Si piston alloys. Materials Science and Engineering: A527(26):7132-7137.
12. Dwivedi.DK.(2003) Sliding temperature and wear behavior of cast Al–Si base alloy. Materials Science and Technology19(8):1091-1096.
13. Chang-Yeol Jeong (2013) High Temperature Mechanical Properties of AlSiMg(Cu) Alloys for Automotive Cylinder Heads. Materials Transactions54(4):588-594
14. Funda Gül Koç. Erdem Karakulak. Rıdvan Yamanoglu. Muzaffer Zeren. Kocaeli Turkey (2016). Mechanical properties of hypoeutectic Al-Ni alloys with Al_3Ni intermetallics)Material Testing58(2):117-121.
15. Mohammed. Farag. Moatasem. M Kh.AM.Omran.M. Atlam AA.(2018) Improvement the mechanical and tribological properties of high temperature Al-Si-Ni alloys JETIR5(6):68-74(ISSN-2349-5162).
16. Yang Yang. Kuilong. Yu. Yunguo Li. Degang Zhao. Xiangfa Liu (2012) Evolution of nickel-rich phases in Al–Si–Cu–Ni–Mg piston alloys with different Cu additions.Materials and Design 33:220-225.

17. Hasan Kayaa. Aynur Akerb.(2016) Effect of Alloying Elements and Growth Rates on Microstructure and Mechanical Properties in the Directionally Solidified Al–Si–X Alloys. Journal of Alloys and Compounds 694:165-170.

18. Riyadh. A Badr.(2017) Effect of Si Addition on Microstructure and Tribological Properties of Al-0.1Mg-0.35Ni-(4,6,8,10) wt %Si Alloy. Materials Science-International Journal of Advancements in Technology 8(4) DOI:10.4172/0976-4860.1000197.

19. Samuel A. Awe. Salem Seifeddine. Anders E. W. Jarfors. Young. C. Lee. Arne K. Dahle.(2017)Development of new Al-Cu-Si alloys for high temperature performance. Advanced Materials Letters.8(6), 695-701.

20. Rajabi.M.Simchi.A.Vahidi.M.Davami.P (2008) Effect of particle size on the microstructure of rapidly solidified Al–20Si–5Fe–2X (X = Cu, Ni, Cr) powder. J of Alloys and Compounds 466(1–2):111-118.

21. Dayanand M Goudar, Veeresh T Magalad, Rajashekar V Kurahatti.(2022).Study of microstructure and tribological behaviour of spray cast high silicon hypereutectic Al-Si alloy. Advances in Materials and Processing Technologies.8:2, 1245-1254.

22. Upadhyaya,A. Mishra.NS. Ojha.SN(1997) Microstructural control by spray forming and wear characteristics of a Babbit alloy.Journal of materials science 32:3227 – 3235.

23. Dayanand M. Goudar. Raju.K.Srivastava.VC.Rudrakshi.GB (2013) Effect of copper and iron on the wear properties of spray formed Al–28Si alloy. Materials & Design, 51:383-390

24. MONOJ BARUAH. ANIL BORAH (2021), Sådhanå (2021) 46:129, Indian Academy of Sciences. https://doi.org/10.1007/s12046-021-01655-8).

25. J. Camarillo-Cisneros, R. Perez- Bustamante,R. Mart´ınez-Sanchez, Al-Si-Cu alloy enhanced to high-temperature application by nickel addition.(2022) Revista Mexicana de F´ısica 68 031004 1–7.

26. Oleg D. Neikov. Atomization and Granulation(2019)Handbook of Non-Ferrous Metal Powders. Technologies and Applications:125-185.

27. Dayanand M. Goudar. Srivastava.VC. Rudrakshi.GB (2017)"Effect of Atomization Parameters on Size and Morphology of Al-17Si Alloy Powder Produced by Free Fall Atomizer. Engineering Journal 21(1):155-168.

28. Jiehua. Li. Fredrik S Hage. Xiangfa Liu. Quentin Ramasse. Peter Schumacher (2016) Revealing heterogeneous nucleation of primary Si and eutectic Si by AlP in hypereutectic Al-Si alloys. Sci Rep 6:25244.https://doi.org/10.1038/srep25244.

29. Rajaram. SG.Kumaran.T.Srinivasa.Rao(2010)High temperature tensile and wear behavior of aluminum silicon alloy. Materials Science and Engineering:A528(1) 247-253.

30. Riahi.AR. Alpas.AT(2001)The role of tribo-layers on the sliding wear behavior of graphitic aluminum matrix composites.Wear, 251(1-12):1396-1407

31. Archard. JF (1953)Contact and rubbing of flat surfaces. J Appl. Phys24:981-988

32. Hirst W.(1957)Proceedings of the Conference on Lubrication and Wear. IMechE, London:674.

33. Ian Hutchings. Philip Shipway(2017)"Tribology Friction and Wear of Engineering Materials. Book (Second Edition)2017 ISBN :978-0-08-100910-9 Published by Elsevier Ltd.

34. Stachowiak.GW. Batchelor. AW(1993) Engineering Tri**b**ology24:1-872 Elsevier

35. Tulika Dixit. Eswar Prasad. K(2022)Effect of Temperature and Sliding Velocity on the Dry Sliding Wear Mechanisms of Boron Modified Ti-6Al-4V Alloys," Lubricants :10. 296. https://doi.org/10.3390/lubricants10110296

36. Dwivedi.DK.Arjun.TS.Thakur.P.VaidyaH.Singh.K (2004) Sliding wear and friction behaviour of Al-18% Si-0.5% Mg alloy. Journal of Materials Processing Technology 152,(30):323–328.

37. Zamri Yusoffa.Shamsul Baharin Jamaludinb. Misbahul Aminc. Politeknik Tuanku Syed Sirajuddin(2010)Tribology and Wear Theory of Aluminium Composites: Review and Discussion..Proceedings of the International Postgraduate Conference on Engineering (IPCE 2010) 16-17, Perlis, Malaysia

38. Razavizadeh. K. Eyre. T S (1982) Oxidative wear of aluminum alloy. Wear79: 325-333

39. K. Razavizadeh, T.S. Eyre(1983) Oxidative wear of aluminium alloys: Part II. Wear ,87(3),261-271. https://doi.org/10.1016/0043-1648(83)90130-8

40. Shivanath. R. Sengupta PK. Eyre.TS (1977) Oxidative wear aluminum-silicon alloys. Br. Foundryman70: 349-356.